LETTERS

Stepwise protein-mediated RNA folding directs assembly of telomerase ribonucleoprotein

Michael D. Stone[1], Mariana Mihalusova[2], Catherine M. O'Connor[5], Ramadevi Prathapam[5], Kathleen Collins[5] & Xiaowei Zhuang[1,3,4]

Telomerase is an essential cellular ribonucleoprotein (RNP) that solves the end replication problem and maintains chromosome stability by adding telomeric DNA to the termini of linear chromosomes[1–3]. Genetic mutations that abrogate the normal assembly of telomerase RNP cause human disease[4]. It is therefore of fundamental and medical importance to decipher cellular strategies for telomerase biogenesis, which will require new insights into how specific interactions occur in a precise order along the RNP assembly pathway. Here we use a single-molecule approach to dissect the individual assembly steps of telomerase. Direct observation of complex formation in real time revealed two sequential steps of protein-induced RNA folding, establishing a hierarchical RNP assembly mechanism: interaction with the telomerase holoenzyme protein p65 induces structural rearrangement of telomerase RNA, which in turn directs the binding of the telomerase reverse transcriptase to form the functional ternary complex. This hierarchical assembly process is facilitated by an evolutionarily conserved structural motif within the RNA. These results identify the RNA folding pathway during telomerase biogenesis and define the mechanism of action for an essential telomerase holoenzyme protein.

Telomerase RNP functions as a multisubunit holoenzyme consisting of telomerase RNA, telomerase reverse transcriptase (TERT) and additional protein cofactors. Catalytically active telomerase enzyme can be reconstituted from RNA and TERT in rabbit reticulocyte lysate (RRL), in which general chaperone activities promote RNP assembly[5,6]. However, the endogenous process of telomerase biogenesis seems to require a more specific assembly pathway[7]. In support of this view, cellular accumulation of telomerase RNP is promoted by a number of specific RNA-binding proteins, including dyskerin in vertebrates, Sm proteins in yeasts, and La-motif proteins in ciliates[8–11]. In the present study we exploited single-molecule fluorescence resonance energy transfer (FRET)[12–14] to explore the mechanism for telomerase RNP biogenesis, using the ciliate *Tetrahymena thermophila* as a model system.

The *Tetrahymena* telomerase RNA is a 159-nucleotide transcript (Fig. 1a) that provides a template for telomere synthesis and functions in adapting the polymerase to its specialized task of reiterative repeat synthesis[15–17]. Using a refined DNA-splinted RNA ligation method[18] (Supplementary Fig. 1) we strategically placed a FRET donor (Cy3) and acceptor (Cy5) flanking the regions important for interaction with TERT and the holoenzyme protein p65, a La-motif protein that promotes telomerase RNP accumulation *in vivo*[11] (Fig. 1a). To facilitate real-time observation of telomerase RNP assembly, RNA was surface-immobilized through an extension of stem II that does not perturb telomerase activity *in vitro* or *in vivo*[19]. Standard DNA primer extension assays performed with both labelled and unlabelled RNA yielded normal profiles of product synthesis (Fig. 1a, inset), indicating that dye labelling did not substantially interfere with RNA function.

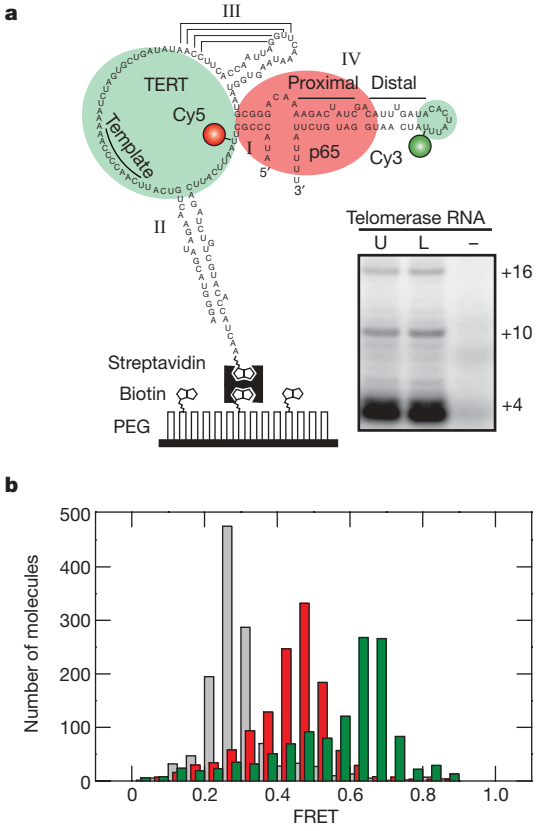

Figure 1 | Telomerase proteins p65 and TERT induce distinct conformational changes in telomerase RNA. a, Full-length telomerase RNA labelled with FRET donor (Cy3) and acceptor (Cy5). RNA molecules were immobilized on a streptavidin-coated surface by a biotin molecule engineered onto an extension of stem II. The interaction sites with p65 (red) and TERT (green) are highlighted[20,24]. Inset: telomerase primer extension assay with dye-labelled (L) and unlabelled (U) RNA or without RNA (−). Numbers at the right indicate the number of nucleotides added to generate each product. **b**, FRET histograms of RNA molecules in the absence of protein (grey bars), the presence of 10 nM p65 (red bars) or 10 nM p65 plus 32 nM $TERT_{1–516}$ (green bars). A peak at FRET = 0 due to the presence of about 30% of molecules without active Cy5 (Supplementary Fig. 2) was removed from these histograms.

[1]Department of Chemistry and Chemical Biology, [2]Department of Molecular and Cellular Biology, [3]Department of Physics, and [4]Howard Hughes Medical Institute, Harvard University, Cambridge, Massachusetts 02138, USA. [5]Department of Molecular and Cell Biology, University of California, Berkeley, California 94720, USA.

The FRET distribution for full-length telomerase RNA showed a single population centred at FRET = 0.29 (Fig. 1b and Supplementary Fig. 2a). Time traces of individual RNA molecules showed a stable FRET level without significant fluctuations except for transient excursions to FRET = 0 due to blinking of the acceptor dye (Supplementary Fig. 3). Addition of purified p65 gave rise to a second population with a steady FRET level at 0.46 (Fig. 1b and Supplementary Fig. 3). Estimating the relative abundance of each population as a function of p65 concentration yielded a non-cooperative p65 binding isotherm with $K = 1.3$ nM (Supplementary Fig. 4), in agreement with ensemble characterization of p65–RNA affinity[20]. Similar results were obtained with telomerase RNA immobilized by a 5′ extension (Supplementary Fig. 5), showing that surface attachment did not perturb the assembly of telomerase RNP. Control experiments designed to prevent a distance change between donor and acceptor dyes upon binding of p65 showed that direct dye–p65 interaction, if present, did not induce any significant change in FRET (Supplementary Fig. 6). Furthermore, binding of p65 did not alter fluorescence intensities from the RNA singly labelled with Cy3 or Cy5 at the same locations (data not shown). Taken together, these results indicate that the p65-induced increase in FRET represents a conformational change within the RNA, wherein the ends of stem I and stem IV are brought closer together in the tertiary RNA fold.

To investigate the assembly of p65–RNA–TERT ternary complex, we used a purified TERT polypeptide containing the amino-terminal 516 amino acids ($TERT_{1–516}$). This polypeptide contains all of the primary sites of RNA–TERT interaction, but unlike the full-length TERT it can be expressed in a soluble recombinant form[20]. Addition of $TERT_{1–516}$ to the p65–RNA complex further shifted the FRET value to a steady value of 0.65 (Fig. 1b and Supplementary Fig. 3), with a binding affinity of $K = 14.4$ nM (Supplementary Fig. 4). The

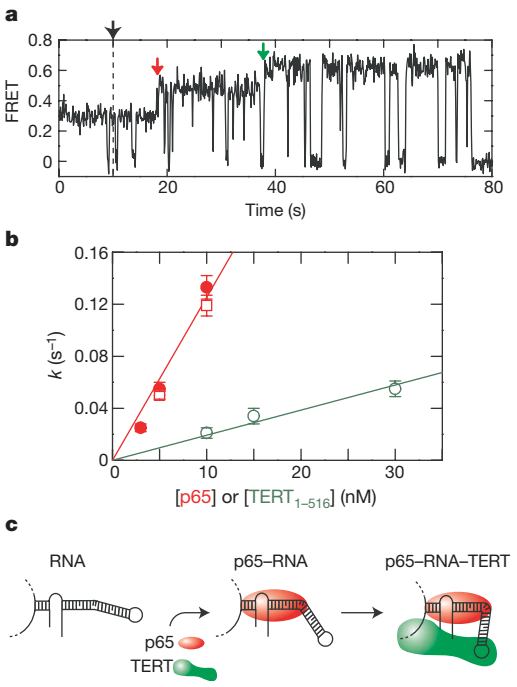

Figure 2 | Real-time assembly of individual telomerase RNP complexes. **a**, A single-molecule FRET trajectory showing hierarchical RNP assembly after the addition (black arrow) of a protein mixture of p65 (10 nM) and $TERT_{1–516}$ (10 nM), characterized by a p65-induced FRET change (red arrow) followed by a second FRET transition after complete assembly of the ternary p65–RNA–$TERT_{1–516}$ complex (green arrow). Excursions to FRET = 0 correspond to blinking of Cy5 (Supplementary Fig. 3) **b**, The conversion rate (k) from FRET = 0.29 to FRET = 0.46 (red) or from FRET = 0.46 to FRET = 0.65 (green) as a function of p65 or $TERT_{1–516}$ concentration, respectively. Open red squares indicate conversion rates measured in the presence of p65 only, and solid red circles indicate those measured in the presence of both p65 and $TERT_{1–516}$. Results are means ± s.e.m. ($n \geq 32$ for all conditions). Linear fits of the data (red and green lines) yield binding rate constants of 1.3×10^7 and 2×10^6 M^{-1} s^{-1} for p65 and $TERT_{1–516}$, respectively. **c**, The interaction of p65 (red) induces compaction in stem I–IV of the RNA, followed by co-assembly with TERT and concomitant additional RNA folding in the ternary complex. The conserved GA bulge introduces a kink in stem IV in the absence of protein[25,26]. The additional bending in stem IV in the presence of proteins is drawn to indicate RNA compaction as measured by FRET, and is not meant to represent a specific structural orientation. Note that tertiary RNA contacts not shown in the model may be formed within the telomerase holoenzyme.

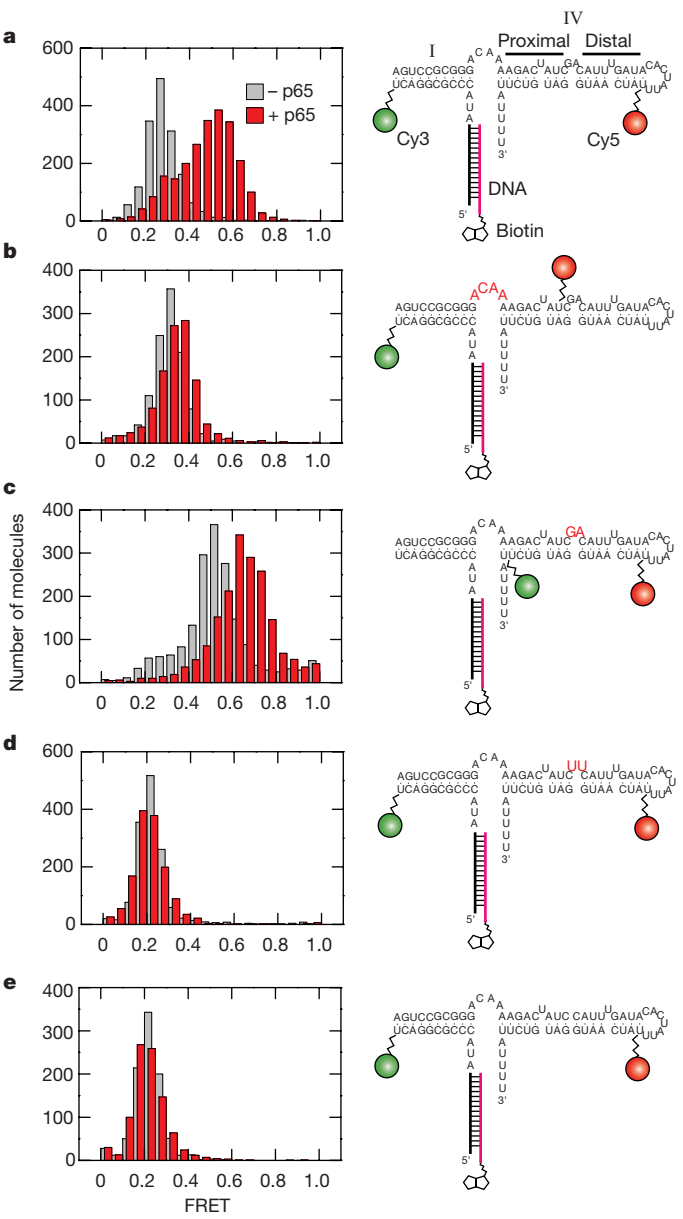

Figure 3 | The p65-induced RNA structural change occurs within stem IV and requires the conserved GA bulge. Schematic illustrations of stem I–IV constructs (right panels) and their corresponding FRET histograms (left panels) in the absence (grey) or presence (red) of p65. **a–c**, Constructs probing conformational change within the entire stem I and stem IV region (**a**), between stem I and proximal stem IV (**b**) and between proximal stem IV and distal stem IV (**c**). **d**, **e**, Constructs probing the role of the GA bulge by substitution (GA→UU) (**d**) and by deletion (ΔGA) (**e**). Stem I–IV constructs were labelled with FRET donor (green spheres) and acceptor (red spheres) and surface-immobilized by means of a 5′ RNA extension (thick black line) annealed to a biotinylated complementary DNA oligonucleotide (pink line).

binding of $TERT_{1–516}$ did not alter fluorescence intensities from RNA singly labelled with Cy3 or Cy5 (data not shown), indicating that the $TERT_{1–516}$-induced FRET change signifies another genuine structural rearrangement in telomerase RNA. FRET measurements on catalytically active telomerase RNPs assembled in RRL with p65 and full-length TERT gave a similar FRET distribution (compare Supplementary Fig. 7a with Fig. 1b), showing that the high FRET conformation (FRET = 0.65) observed in the p65–RNA–$TERT_{1–516}$ ternary complex represents the RNA structure in the functional enzyme.

The distinct FRET signatures of the telomerase RNA alone, the p65–RNA complex and the p65–RNA–$TERT_{1–516}$ ternary complex allowed us to examine the assembly of individual telomerase RNP particles in real time. We therefore added protein mixtures containing both p65 and $TERT_{1–516}$ to telomerase RNA and monitored the FRET signal of individual RNA molecules during the assembly process. Most assembly trajectories (74%, $n = 173$) displayed a prominent kinetic intermediate with FRET = 0.46, equivalent to that measured from p65–RNA complex, before attaining a final state with FRET = 0.65 indicative of the p65–RNA–TERT ternary complex (Fig. 2a and Supplementary Fig. 3b). The remaining minor fraction of assembly trajectories exhibited less defined intermediates with irregular FRET fluctuations (Supplementary Fig. 8). The fraction of molecules assembled through the well-defined two-step (0.29→0.46→0.65) pathway did not vary substantially with altered ratios of p65 to $TERT_{1–516}$ concentrations (at p65-to-$TERT_{1–516}$ ratios of 1:1, 1:3 and 1:10, the proportions were 73% ($n = 37$), 76% ($n = 101$) and 69% ($n = 35$), respectively). The rates of conversion from FRET = 0.29 to FRET = 0.46 and from FRET = 0.46 to FRET = 0.65 increased linearly with p65 and $TERT_{1–516}$ concentrations, respectively (Fig. 2b).These results indicate a possible hierarchical telomerase assembly process directed by sequential steps of protein-induced RNA folding: assembly is initiated by p65 binding, stabilizing a RNA structural intermediate, which in turn promotes the functional co-assembly of TERT with telomerase RNA (Fig. 2c).

To characterize the p65-induced assembly intermediate structurally, we generated a series of truncated constructs composed of telomerase RNA stems I and IV, harbouring the primary p65 interaction sites[20] (Fig. 3). When FRET donor and acceptor were incorporated in stem I and distal stem IV (approximating the labelling sites in the full-length RNA construct), we observed a significant increase in FRET when p65 bound (Fig. 3a), which is consistent with results described above (Fig. 1b). Experiments with FRET donor and acceptor relocated to flank the ACAA linker (Fig. 3b) or the dinucleotide GA bulge (Fig. 3c) indicated that the primary p65-induced structural rearrangement occurs between proximal and distal stem IV linked by the GA bulge rather than between stem I and stem IV. Furthermore, substitution (GA→UU; Fig. 3d) or deletion (ΔGA; Fig. 3e) of the GA bulge abolished any stable p65-induced FRET change. At the concentration of p65 used here (30 nM), most RNA molecules were bound to p65 (Supplementary Fig. 9). Thus, the p65-induced RNA conformational change occurs within stem IV and requires the central stem IV GA bulge, which is conserved across all *Tetrahymena* species[21].

To probe whether the p65-induced RNA conformation is an essential intermediate during hierarchical telomerase RNP biogenesis, we compared the assembly observations described above with reactions that lacked p65 or lacked the GA bulge in telomerase RNA. Telomerase RNA in the presence of $TERT_{1–516}$ alone did not yield the stable high-FRET state (FRET = 0.65) observed for the p65–RNA–$TERT_{1–516}$ ternary complex (compare Fig. 4a with Fig. 1b). Instead, the FRET trajectories showed characteristic fluctuations with amplitudes and rates that were independent of $TERT_{1–516}$ concentration (1–100 nM) (Fig. 4b and Supplementary Fig. 10), indicating that the FRET dynamics were not due to the repetitive binding and dissociation of protein. The fraction of molecules showing such fluctuations increased with the concentration of $TERT_{1–516}$ (data not shown), with an affinity comparable to the previously determined value for telomerase RNA and $TERT_{1–516}$ (ref. 20). These results show that the RNA fold in the RNA–$TERT_{1–516}$ complex is structurally different from that in the p65–RNA–$TERT_{1–516}$ ternary complex. Addition of p65 to preformed RNA–$TERT_{1–516}$ complexes recovered the stable high-FRET conformation (data not shown), indicating that p65 might be able to rescue misassembled RNA–TERT complexes by directing productive interactions between TERT and telomerase RNA. Furthermore, p65 substantially stimulated the complex formation and catalytic activity of telomerase RNPs reconstituted in RRL (Supplementary Fig. 7). The role of p65 therefore cannot be fully recapitulated by heterologous factors within RRL.

When p65 was added to full-length telomerase RNA lacking the GA bulge, no stable FRET change was observed (Fig. 4c). Instead, the FRET traces visited a higher FRET state only transiently (Fig. 4d), with a rate independent of p65 concentration (data not shown), indicating that disruption of the GA bulge might render the stem IV region too rigid to be folded by p65 in a stable manner. Subsequent addition of $TERT_{1–516}$ did not substantially change the FRET dynamics or induce the FRET = 0.65 conformation indicative of the functional p65–RNA–TERT complex (compare Fig. 4c with

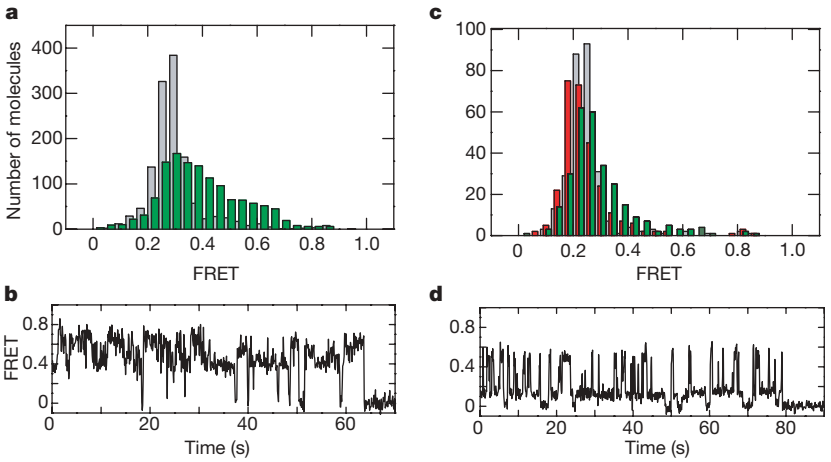

Figure 4 | The p65 protein and conserved GA bulge in stem IV of telomerase RNA are required for telomerase assembly. a, FRET histograms of full-length RNA in the absence (grey bars) or presence (green bars) of 10 nM $TERT_{1–516}$. **b**, A single-molecule FRET trajectory of telomerase RNA in the presence of 10 nM $TERT_{1–516}$. **c**, FRET histograms of full-length RNA lacking the GA bulge (ΔGA) in the absence of protein (grey bars), in the presence of 10 nM p65 (red bars) or in the presence of 10 nM p65 plus 30 nM $TERT_{1–516}$ (green bars). **d**, A single-molecule FRET trajectory of ΔGA RNA in the presence of 10 nM p65.

Fig. 1b). Furthermore, *in vivo* deletion of the conserved GA bulge or its replacement with UU prevented the incorporation of telomerase RNA into a stable RNP, resulting in the failure of these RNA variants to accumulate relative to endogenous telomerase RNA (Supplementary Fig. 11). Taken together, these results show that the p65-induced RNA conformational change is critical for formation of the native p65–RNA–TERT complex.

Thus, our experiments directly show a hierarchical assembly mechanism for telomerase RNP in which the protein subunits mould a specific RNA tertiary structure in a stepwise fashion. First, the telomerase holoenzyme protein p65 induces a marked structural change within the stem IV region of the RNA, a domain important for processive telomere synthesis[15–17]. This stable structural rearrangement strictly requires the central stem IV GA bulge, accounting for the phylogenetic conservation of this sequence motif. Second, the RNA conformation in the p65–RNA complex is further altered by binding of TERT, resulting in a compact RNA tertiary fold within the functional telomerase RNP. By monitoring the assembly of individual RNP complexes in real time, we showed that the p65-induced RNA conformation is a fundamental structural intermediate during hierarchical telomerase assembly. These results provide a likely mechanism for telomerase RNP assembly *in vivo*, in which a holoenzyme protein repositions distant RNA-binding sites for TERT, promoting the correct co-assembly of the catalytic subunit TERT with telomerase RNA (Figs 1a and 2c). Consistent with this notion, removal of p65 (ref. 11) or mutation of the GA bulge prevents the incorporation of telomerase RNA into a stable RNP *in vivo* (Supplementary Fig. 11). An analogous hierarchical biogenesis pathway has been proposed for the ribosome[22,23], which contains an RNA rather than a protein catalytic centre. Hierarchical steps of protein-mediated RNA folding might therefore represent a general assembly strategy for cellular RNPs, providing multiple layers of control to circumvent the formation of long-lived misassembled intermediates.

METHODS

RNA and protein preparation. Full-length FRET-labelled RNAs were prepared by a refined DNA-splinted RNA ligation method detailed in Supplementary Methods and Supplementary Fig. 1. The preparation of truncated RNA constructs is described in Supplementary Methods. Histidine-tagged p65 and $TERT_{1–516}$ proteins were expressed and purified from *E. coli* as described[20].

Single-molecule FRET. Single-molecule FRET measurements were performed as described in Supplementary Methods. The FRET value is defined as $I_A/(I_A + I_D)$, where I_D and I_A are the fluorescence intensities measured in the donor and acceptor channels, respectively.

RRL reconstitution of telomerase RNP and *in vivo* RNA accumulation assays. Protein expression in RRL was performed by standard methods (Supplementary Methods) with the pCITE plasmid system as described[16]. *In vivo* telomerase RNA accumulation assays are described in Supplementary Methods.

Received 18 September 2006; accepted 15 January 2007.
Published online 25 February 2007.

1. Greider, C. W. & Blackburn, E. H. Tracking telomerase. *Cell* **116,** S83–S86 (2004).
2. Cech, T. R. Beginning to understand the end of the chromosome. *Cell* **116,** 273–279 (2004).
3. Collins, K. The biogenesis and regulation of telomerase holoenzymes. *Nature Rev. Mol. Cell Biol.* **7,** 484–494 (2006).
4. Wong, J. M. & Collins, K. Telomere maintenance and disease. *Lancet* **362,** 983–988 (2003).
5. Weinrich, S. L. *et al.* Reconstitution of human telomerase with the template RNA component hTR and the catalytic protein subunit hTRT. *Nature Genet.* **17,** 498–502 (1997).
6. Holt, S. E. *et al.* Functional requirement of p23 and Hsp90 in telomerase complexes. *Genes Dev.* **13,** 817–826 (1999).
7. Harrington, L. Biochemical aspects of telomerase function. *Cancer Lett.* **194,** 139–154 (2003).
8. Mitchell, J. R., Wood, E. & Collins, K. A telomerase component is defective in the human disease dyskeratosis congenita. *Nature* **402,** 551–555 (1999).
9. Seto, A. G., Zaug, A. J., Sobel, S. G., Wolin, S. L. & Cech, T. R. *Saccharomyces cerevisiae* telomerase is an Sm small nuclear ribonucleoprotein particle. *Nature* **401,** 177–180 (1999).
10. Aigner, S., Postberg, J., Lipps, H. J. & Cech, T. R. The *Euplotes* La motif protein p43 has properties of a telomerase-specific subunit. *Biochemistry* **42,** 5736–5747 (2003).
11. Witkin, K. L. & Collins, K. Holoenzyme proteins required for the physiological assembly and activity of telomerase. *Genes Dev.* **18,** 1107–1118 (2004).
12. Stryer, L. & Haugland, R. P. Energy transfer: a spectroscopic ruler. *Proc. Natl Acad. Sci. USA* **58,** 719–726 (1967).
13. Ha, T. *et al.* Probing the interaction between two single molecules: fluorescence resonance energy transfer between a single donor and a single acceptor. *Proc. Natl Acad. Sci. USA* **93,** 6264–6268 (1996).
14. Zhuang, X. Single-molecule RNA science. *Annu. Rev. Biophys. Biomol. Struct.* **34,** 399–414 (2005).
15. Sperger, J. M. & Cech, T. R. A stem-loop of *Tetrahymena* telomerase RNA distant from the template potentiates RNA folding and telomerase activity. *Biochemistry* **40,** 7005–7016 (2001).
16. Lai, C. K., Miller, M. C. & Collins, K. Roles for RNA in telomerase nucleotide and repeat addition processivity. *Mol. Cell* **11,** 1673–1683 (2003).
17. Mason, D. X., Goneska, E. & Greider, C. W. Stem-loop IV of *Tetrahymena* telomerase RNA stimulates processivity in *trans*. *Mol. Cell. Biol.* **23,** 5606–5613 (2003).
18. Moore, M. J. & Query, C. C. Joining of RNAs by splinted ligation. *Methods Enzymol.* **317,** 109–123 (2000).
19. Cunningham, D. D. & Collins, K. Biological and biochemical functions of RNA in the *Tetrahymena* telomerase holoenzyme. *Mol. Cell. Biol.* **25,** 4442–4454 (2005).
20. Prathapam, R., Witkin, K. L., O'Connor, C. M. & Collins, K. A telomerase holoenzyme protein enhances telomerase RNA assembly with telomerase reverse transcriptase. *Nat. Struct. Mol. Biol.* **12,** 252–257 (2005).
21. Ye, A. J. & Romero, D. P. Phylogenetic relationships amongst tetrahymenine ciliates inferred by a comparison of telomerase RNAs. *Int. J. Syst. Evol. Microbiol.* **52,** 2297–2302 (2002).
22. Adilakshmi, T., Ramaswamy, P. & Woodson, S. A. Protein-independent folding pathway of the 16S rRNA 5′ domain. *J. Mol. Biol.* **351,** 508–519 (2005).
23. Talkington, M. W., Siuzdak, G. & Williamson, J. R. An assembly landscape for the 30S ribosomal subunit. *Nature* **438,** 628–632 (2005).
24. O'Connor, C. M., Lai, C. K. & Collins, K. Two purified domains of telomerase reverse transcriptase reconstitute sequence-specific interactions with RNA. *J. Biol. Chem.* **280,** 17533–17539 (2005).
25. Richards, R. J. *et al.* Structural study of elements of *Tetrahymena* telomerase RNA stem–loop IV domain important for function. *RNA* **12,** 1475–1485 (2006).
26. Chen, Y. *et al.* Structure of stem-loop IV of *Tetrahymena* telomerase RNA. *EMBO J.* **25,** 3156–3166 (2006).

Supplementary Information is linked to the online version of the paper at www.nature.com/nature.

Acknowledgements We thank M. Bates for LabView software for data acquisition. This work was supported in part by the NIH and the Packard Foundation (X.Z.), and the NIH (K.C.). X.Z. is a Howard Hughes Medical Institute investigator. M.D.S. is a. NIH Ruth L. Kirschstein NSRA Fellow.

Author Information Reprints and permissions information is available at www.nature.com/reprints. The authors declare no competing financial interests. Correspondence and requests for materials should be addressed to X.Z. (zhuang@chemistry.harvard.edu).